Self organisation of plasma turbulence: impact on radial correlation lengths

Philippe Ghendrih, , Guilhem Dif-Pradalier, Claudia Norscini, Thomas Cartier-Michaud, Damien Estève, Xavier Garbet, Virginie Grandgirard, Guillaume Latu, Chantal Passeron, Yanick Sarazin

CEA, IRFM, F-13108 Saint-Paul-lez-Durance, France

E-mail: philippe.ghendrih@cea.fr

Abstract. The empirical scaling law used to support the projected ITER performance [1, 2] in analysed to determine the control parameters that must be considered in gyrokinetic simulations. The results of such an analysis are contradictory and do not appear to fit with present evidence from gyrokinetic simulations. Analysing the dependence of the correlation length on the ρ_* parameter, we show that local values of the correlation length are governed by the shearing effect of the corrugation patterns, but that coarse graining this value, in time, radially or poloidally does not allow one to recover this match. A comparison to the scaling law must then rely on the scaling properties of the Probability Density Function of the correlation length that is found to exhibit heavy tails with algebraic decay.

1. Introduction

The scaling law for the energy confinement time has been an area of very important research activity that both summarises the experimental effort and has allowed one to design devices with a prescribed fusion performance as in the case of ITER [3, 1, 2]. A key commitment of large scale computing with gyrokinetics models [4] is to back such a scaling law [5, 6, 7] and increase our confidence by combining understanding and precise predictions to be challenged by experimental investigation [8, 9, 10, 11].

As it stands the reference scaling law need clarification. The issue of the β dependence is often alluded to [12, 13, 14]. Here we concentrate on the leading dependence, namely the ρ_* dependence [14, 2], the only to exhibit a mass dependence. Some concern has already been pointed out regarding the isotope effect that appears to depart from that expected from the ρ_* effect[15, 16, 17]. More recent theoretical results on the change of transport from Bohm to gyro-Bohm when $1/\rho_*$ exceeds 300 [5, 6, 18] appear to be in contradiction with the more gyro-Bohm like feature of the empirical scaling law. Indeed, the present machine pool used to build the experimental evidence should exhibit a significantly weaker dependence on ρ_* than it actually does. This aspect is presently being revisited by scaling the heating power in the simulations with ρ_* [19]. Further effort should help in clarifying both the expected ρ_* and mass dependences in gyrokinetic flux-driven simulations [20, 21, 22, 23]. Also, a quite important issue is to bridge the key features of the scaling law with the meso-scale structures, such as avalanches


Content from this work may be used under the terms of the Creative Commons Attribution 3.0 licence. Any further distribution of this work must maintain attribution to the author(s) and the title of the work, journal citation and DOI.
Published under licence by IOP Publishing Ltd

Table 1. Exponents of the energy confinement time scaling

τ_0	α_i	α_n	α_p	α_r	α_a	α_k	α_m	α_b
0.0562	0.93	0.41	0.69	1.97	0.58	0.78	0.19	0.15

[24, 25, 26, 27, 28] and corrugations [29, 30, 31, 32], that are believed to play a strong role in turbulent transport regulation [33].

The scope of our confinement analysis with global flux driven simulations is to determine the key control parameters and the physics that drive these dependences. In the framework of scaling laws, which hold over a couple of decades, we rely on the assumption that all details are not important and that confinement properties are based on a few robust features. Should this not be the case, or should the simple scaling that is observed be the result of competing mechanisms that tend to cancel out, would be an outstanding but quite problematic result for fusion. Whatever, stepping up our present predictive capability with global flux-driven simulations is a first priority and the scope of the present work.

The paper is organised as follows. In Section 2 we revisit the conversion of the scaling law for the energy confinement time from the so-called engineer parameters to dimensionless parameters. Our interest is to highlight the expressions that allow one to compute the exponents of the control parameters that are relevant to gyrokinetic simulation. The computation of the correlation length in a GYSELA [20] simulation evolving towards global balance between the heating source and the exhaust flux at the outer radius is described in Section 3. We then show in Section 4 that the correlation length is strongly related to local effects in time, radius and poloidal angle. The latter effect appears to stem from the interplay between corrugations and avalanches that self-consistently determine the transport level. The relevance of coarse graining action to extract from the broad Probability Density Function a relevant correlation length is discussed there. Finally, Section 5, dedicated to the Discussion and Conclusion, closes the paper.

2. Energy confinement scaling laws

The guideline for ITER design is the scaling law for the energy confinement τ_E built with an international data base of experimental results [2]. In its standard form it is expressed in terms of products of so-called engineer parameters at some power:

$$\tau_E = \tau_0 \;\; I_{MA}^{\alpha_i} \;\; n_{19}^{\alpha_n} \;\; P_{MW}^{-\alpha_p} \;\; R_{SI}^{\alpha_r} \;\; A^{-\alpha_a} \;\; \kappa_a^{\alpha_k} \;\; M^{\alpha_m} \;\; B_{SI}^{\alpha_b} \tag{1}$$

The values of the various exponents are given in table 1 and the subscripts indicate the normalisation of the various terms. Strangely enough, some parameters are already dimensionless such as the plasma elongation κ_a, the plasma aspect ratio A and the mass number M which is the mass of the ion species normalised by the nucleon mass. In this formulation, the various exponents, the α's, are defined in such a way that they are positive. The chosen parameters for this scaling law are the plasma current I, the plasma density n, the heating power P, the major radius R and the magnetic field amplitude B. This combination of parameters at various powers must yield by definition a time unit for τ_E, the so-called Kadomtsev constraint [34]. One the obtains the following relationship between the exponents:

$$5\ \alpha_b = 3\alpha_p + 4\alpha_r - \Big(8\alpha_n + \alpha_i + 5\Big) \tag{2}$$

This relation is satisfied by the coefficients of table 1 within less than 1 %. It is to be noted that the results appears as a difference between two large values that weigh more than 13 times their

difference, a feature that is prone to error amplification. This done, the scaling law is expressed in terms of dimensionless control parameters, namely ρ_*, β and ν_*. We only address here the ρ_* dependence, this parameter being defined as:

$$\rho_* = \frac{\rho_p}{a} = \frac{(T/m_p)^{1/2}}{a\ \Omega_p} \tag{3}$$

where a is the plasma minor radius, $a = R/A$, and where ρ_p, m_p and Ω_p are the proton Larmor radius, mass and cyclotron frequency respectively. The temperature T is the volume-average thermal energy per particle. The ρ_* parameter is akin to the Reynolds number insofar that it accounts for the number of degrees of freedom in the system. However, this estimate only takes into account the effect of the temperature, of the magnetic field and that of the size of the device. The mass effect is not taken into account in this definition. When switching to dimensionless parameters one finds:

$$\Omega_p \tau_E \propto \nu_*^{\alpha_\nu}\ \rho_*^{-\alpha_\rho}\ \beta^{\alpha_\beta}\ q_{cyl}^{\alpha_{qcyl}}\ A^{\alpha_A}\ (q/q_{cyl})^{\alpha_q}\ \kappa_a^{\alpha_\kappa}\ M^{\alpha_M} \tag{4}$$

In this expression the dependence on q_{cyl} the cylindrical value of the safety factor essentially accounts for the plasma current dependence and directly impacts the dependence on the aspect ratio A. The dependence on (q/q_{cyl}) is related to shaping properties similarly to that on the elongation κ. The exponents for ν_* is of order zero while that of β is of order minus one, hence a rather severe degradation of the confinement with β, while α_ρ is found to be:

$$\alpha_\rho = \frac{6\Big(\alpha_i + \alpha_r\Big) - 2\ \alpha_n - 18\ \alpha_p}{5(1-\alpha_p)} \tag{5}$$

Given the data from table 1, one finds $\alpha_\rho \approx 2.68$ quite close to the value 3 of the gyro-Bohm scaling. Similarly one obtains:

$$\alpha_{qcyl} = \frac{\alpha_r - 2\alpha_n - 3\alpha_p - 4\alpha_i}{5(1-\alpha_p)} \tag{6}$$

$$\alpha_A = \frac{-\alpha_i + 3\alpha_r - 2\alpha_n - 5\alpha_p - 2\alpha_a}{2(1-\alpha_p)} \tag{7}$$

$$\alpha_M = \frac{\alpha_m}{1-\alpha_p} \tag{8}$$

which yields: $\alpha_{qcyl} \approx -2.99$, $\alpha_A \approx -0.73$, $\alpha_M \approx 0.61$. In such an analysis, small q_{cyl}, small A and large M are favourable. The largest dependence in the confinement scaling law is thus found to be approximately $(q_{cyl}\ \rho_*)^{-3}$, hence gyro-Bohm like regarding ρ_*.

In this framework, where transport is implicitly considered to be diffusive, one readily understands the exponent within the random-walk paradigm. Heat is then described to experience a random walk from the plasma core, where the heat source is located, to the heat sink at the plasma boundary. Within this $1D$ description the confinement time takes the form $\tau_E = \tau_{rw} N_*^2$, where N_* is the number of steps between the core and the edge, and τ_{rw} is the characteristic time of one step. For electrostatic turbulence in magnetised plasmas, the eddy size, hence the step of the random walk scales like ρ with characteristic velocity v_E the $E \times B$ electric drift velocity. As a consequence, one obtains $N_* = a/\rho$, and, given the drift ordering, $\tau_{rw} = \rho/v_E = a/c$, where c is the thermal velocity. Given $\rho_{s*} = \rho/a$ where $\rho_{s*} = \sqrt{M}\rho_*/Z$ is

species dependent (hence the subscript s):

$$N_* = \frac{1}{\rho_{s*}} = \frac{a\,\Omega}{(T/(Mm_p))^{1/2}} = \frac{Z\sqrt{M}}{M}\frac{a\,\Omega_p}{(T/m_p)^{1/2}} == \frac{Z}{\sqrt{M}}\frac{1}{\rho_*} \quad (9)$$

$$\tau_{rw} = \frac{1}{\Omega_p}\frac{M}{Z}\frac{1}{\rho_{s*}} = \frac{1}{\Omega_p}\frac{M}{Z}N_* \quad (10)$$

One thus obtains $\Omega_p\tau_E = N_*^3 M/Z$. In this expression, the confinement time depends on the number of steps N_* which is an effective measure of the number of degrees of freedom. Following this understanding of the ρ_* dependence, the scaling of the confinement time should take the form $\Omega_p\tau_E \propto N_*^{\alpha_\rho} M^{\alpha_{sM}}$. The other dimensionless control parameters do not depend on the mass so that the new exponent for the mass dependence α_{sM} is then:

$$\alpha_{sM} = \frac{\alpha_m}{1-\alpha_p} + \frac{\alpha_\rho}{2} \approx 1.95 \quad (11)$$

This introduces therefore a much stronger mass ratio M dependence than would be expected. In flux driven gyrokinetic simulations, one must also relate the injected power P to the dimensionless parameters. The power must then scale with ρ_* as well as with M. The ρ_* dependence stems from the increased volume to heat, scaling typically like ρ_*^{-3} balanced by the improved confinement at smaller ρ_*. The isotope effect is only governed by its impact on the confinement time. One thus obtains:

$$P \propto \rho_*^{-p_\rho} M^{-\alpha_M} \quad ; \quad p_\rho = 18/5 - \alpha_p \quad (12)$$

The required power increases with $1/\rho_*$ with an exponent $p_\rho \approx 0.92$ [19] while the isotope effect allows one to reduce the power with increasing M to achieve a similar plasma performance. It is to be underlined that this increase is less that required to maintain a power density or a heat flux due to the confinement enhancement with $1/\rho_*$.

The latter result [19] is important when discussing the crossover from Bohm to gyro-Bohm as $1/\rho_*$ exceeds 300 as reported in gyrokinetic simulations [5, 6, 18]. Indeed, since the devices used in the scaling law database range from Compass with $1/\rho_* \approx 50$ to JET $1/\rho_* \approx 300$, one would then predict that the global energy confinement time to do no better than Bohm when only the size of the device is scanned. The gyrokinetic codes, used to shed light and build confidence in the empirical scaling law, must therefore be run in carefully determined scans. In the case of global and flux driven codes, the simulations can be addressed in the same framework as the experiments [19].

The scope of the following analysis is to address the issue of the ρ_* scaling, including the mass ratio dependence with the GYSELA code. However, given the computation cost to reach a confinement time with global, flux driven, gyrokinetic simulations, our approach is based on analysing the local features of turbulence during the transient towards plasma thermal equilibrium. Of particular interest, is to identify the characteristic step and duration of such a step in the transport process [35]. The underlying assumption is that turbulence has reached equilibrium locally so that standard measurements such as that of the correlation length L_c or correlation time τ_c are relevant of the statistical steady state. Alternatively, their evolution would also be indicative of the global feature of turbulence. Finally, assuming that the correlation length and time are a measure of the random walk step and characteristic time then allows one to link the local and global properties of turbulent transport. With respect to the scaling issue we then expect L_c/ρ_p to scale between ρ/ρ_p and $(\rho/\rho_p)^{1/2}\rho_*^{-1/2}$ while $\tau_c\ c_p\ M^{1/2}/a$ would scale

from a constant to being proportional to $(\rho/\rho_p)^{1/2}\rho_*^{-1/2}$. Here $c_p = \rho_p\ \Omega_p$ and $\rho_p/\rho = \rho_*\ N_*$. The gyro-Bohm limit would correspond to $L_c/\rho_p \propto \rho/\rho_p$ and $\tau_c\ c_p\ M^{1/2}/a \propto 1$ while the Bohm limit would be met with either $L_c/\rho_p \propto (\rho/\rho_p)^{1/2}\rho_*^{-1/2}$ and $\tau_c\ c_p\ M^{1/2}/a \propto 1$ or $L_c/\rho_p \propto \rho/\rho_p$ and $\tau_c\ c_p\ M^{1/2}/a \propto (\rho/\rho_p)^{1/2}\rho_*^{-1/2}$. Such an approach of confinement properties matches that in experiments where the measurement of the turbulent correlations, hence local properties, complete the global measurements.

3. Correlation length of the electric potential fluctuations in a slowly evolving temperature profiles

In this Section we analyse the $1/\rho_* = 300$ GYSELA simulation described in [31] with fixed density and constant heating source. Profiles close to experimental ones from Tore Supra shot TS45511 have been used, in particular ν_* that weighs the normalised collision term figure 1, the safety factor q figure 1, the density profile figure 2, which is constant in time (given the assumption of adiabatic electrons), and the initial ion temperature profile figure 2. The safety factor, close to one towards the core increases monotonically to $r/a = 1$ where it reaches a relatively large value, $q_a \approx 4$. The circular cross section of Tore Supra are convenient to reduce the simulation cost. Still, in the present paper, the chosen ρ_*, $\rho_* = 1/300$, is larger than that of the Tore Supra shot, $\rho_* \approx 1/450$. The temperature profile is observed to evolve on long time

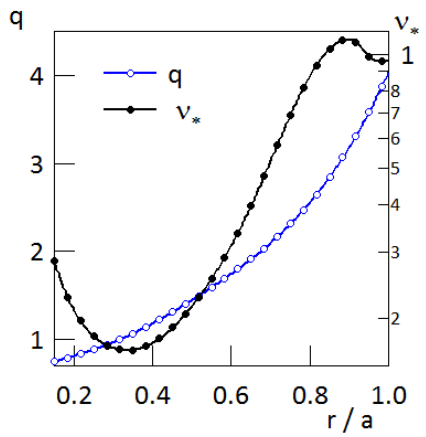

Figure 1. Safety factor q and collisionality ν_* profiles used in the simulation.

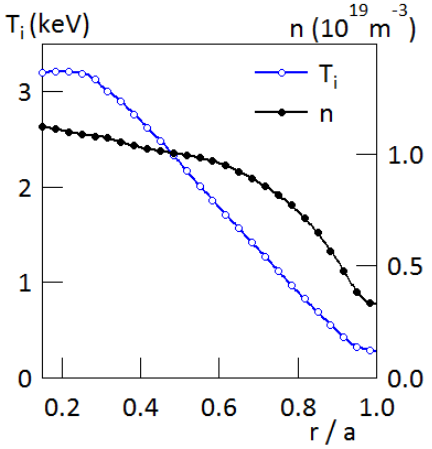

Figure 2. Density n and initial temperature T_i profiles used in the simulation.

scales, figure 3, with a broad region at constant temperature gradient, figure 4. In this paper we concentrate on the radial correlation length of the electric potential $\phi(r, \theta, \varphi = 0, t)$. In practise, the available data is given at an arbitrary value of the toroidal angle φ. As explained in [31], the poloidal average of ϕ is taken as a proxy for the flux averaged potential, an approximation that has been tested to be quite accurate. We thus determine the potential fluctuations as $\tilde{\phi}(r, \theta, \varphi = 0, t) = \phi(r, \theta, \varphi = 0, t) - < \phi(r, \theta, \varphi = 0, t) >_{\theta,[t]}$. Here the averaging operator <> is applied over all poloidal angles θ and for shifting time windows indicated by the notation $[t]$. This allows one to remove the slowly varying features of the electrostatic potential. The time window is 129 points in time long, the delay between consecutive times being $0.8a/c_0$. This time window has been chosen as above the minimum time window providing correct values of L_c. Depending on the cases, we have allowed for an overlap of the times windows, typically of 50 %, but also 95 % and the reference case at 0 %. The time window is centred on the

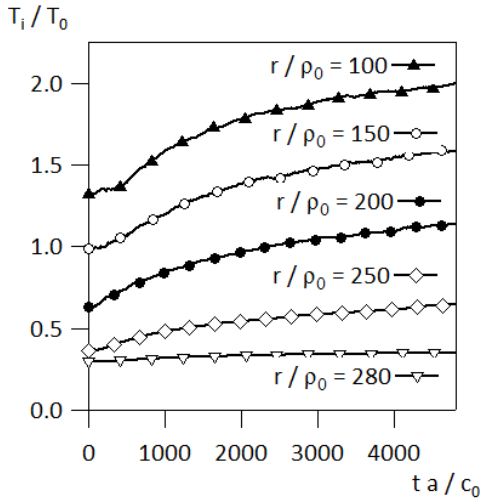

Figure 3. Time trace of the ion temperature at various radial positions.

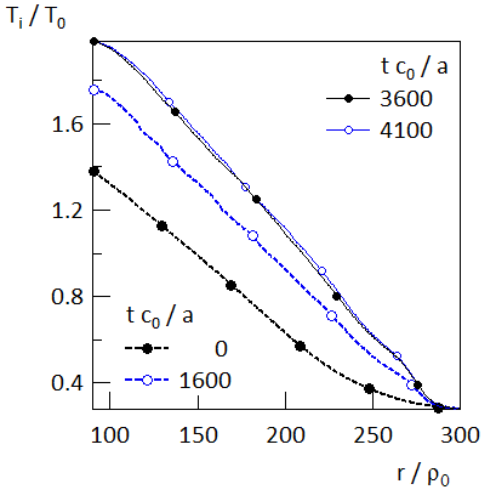

Figure 4. Temperature profiles in the gradient region displaying the gradual increase of the temperature gradient.

time of reference t of the expression of $\tilde{\phi}$. Due to the high frequency modulation in time of the electrostatic potential and the comparatively small variation in radius, the radial average value is also removed so that the field of interest is $\delta\phi = \tilde{\phi} - <\tilde{\phi}>_r$, see figure 5. In the case of adiabatic electrons, this field then corresponds to electron density fluctuations. The correlation function is defined as:

$$C_\phi(r,\theta,t,\delta r) = \frac{<\delta\phi(r,\theta,t)\ \delta\phi(r+\delta r,\theta,t)>_{[t]}}{\left(<\delta\phi(r,\theta,t)^2>_{[t]}\ \ <\delta\phi(r+\delta r,\theta,t)^2>_{[t]}\right)^{1/2}} \tag{13}$$

It decays close to exponentially from its maximum at 1 for $\delta r = 0$. The correlation length is defined here such that $C_\phi(r,\theta,t,\delta r = L_c) = 1/2$. The result of the calculation is then a

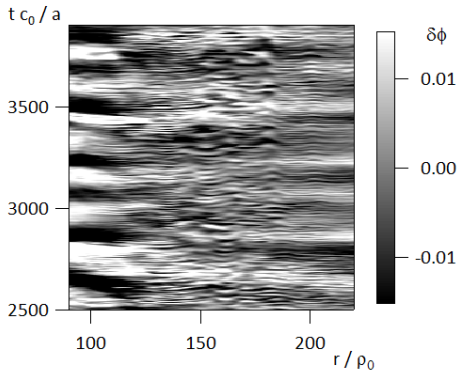

Figure 5. Fluctuations of the electric potential contour map akin to electron density fluctuations.

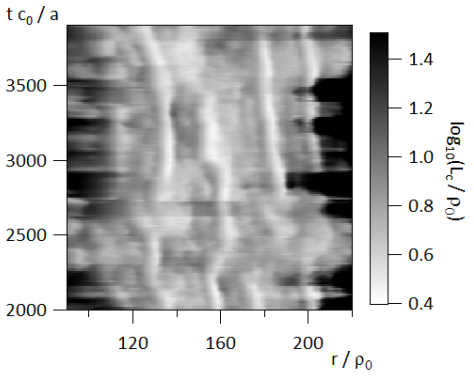

Figure 6. Contour map of the connection length L_c, computed as the local PDF average.

3D map of the correlation length depending on time, poloidal angle and radius. Taking data

within various intervals of time, poloidal angle and even radius provides a way to build Probability Density Functions from which one can compute moments and in particular the mean value.

As a first example of the result of the calculation, the mean value of the correlation length in the low field side region $0 \leq \theta \leq \pi/4$ ($\theta = 0$ in the midplane low field side) is shown on figure 6. From the time trace of the radial profile of $\delta\Phi$, figure 5, one can identify three regions. Towards the plasma centre with $r \leq 120\ \rho_0$, a large amplitude and low frequency activity appears to dominate the fluctuation behaviour. On the correlation length counterpart, figure 6, it is characterised by large values of the correlation length $L_c \geq 10$. Towards the outer radius, $r \geq 200\ \rho_0$, in a radial region where turbulence appears to take the form of low frequency streamer like structures, an abrupt transition is observed. It corresponds in fact to a region where $L_c \geq 40$ which is the upper limit used in the calculation of the correlation function $C_\phi(r, \theta, t, \delta r)$. It is interesting to note that the boundary of these two regions appears to fluctuate in time with both high and meso frequencies [36]. In the correlation function contour plot, and between these two radial boundaries, one can readily identify a pattern of small L_c values that appears to be radially localised and evolve slowly in time. With "good eyes", one can identify a similar pattern in the $\delta\phi$ contour plot, figure 5.

Should L_c scale with ρ, hence with $\sqrt{T_i}$ one would expect a ratio of L_c of typically 1.6 between the inner and outer radius values of the region that is analysed. Such a trend is not readily observed in the simulation data.

The statistical analysis of L_c is first addressed with Probability Density Function (PDF). On

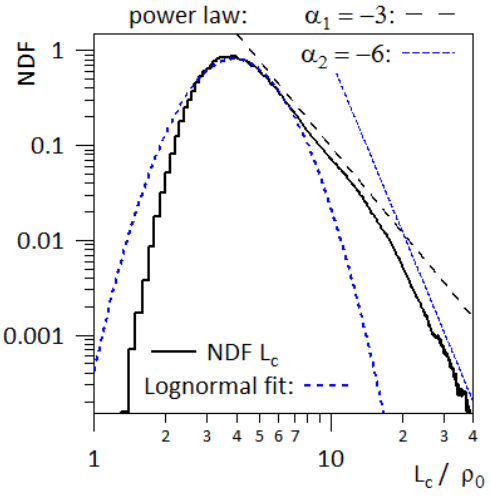

Figure 7. PDF of L_c (not normalised to unity integral), Note the loglog axis.

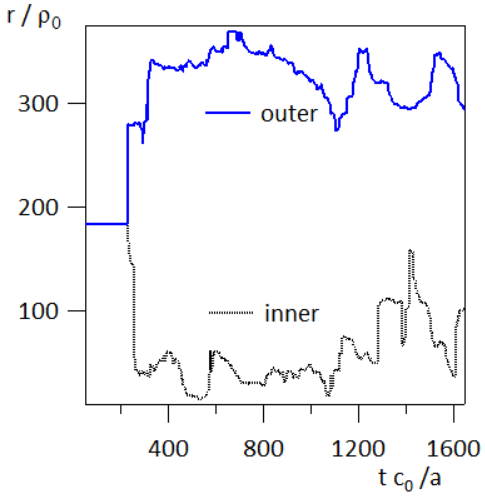

Figure 8. Inner and outer boundary of the region such that $L_c \leq 40\ \rho_0$.

figure 7 the PDF is plotted in a log-log scale which means that a PDF with parabolic shape corresponds to a lognormal distribution. The PDF for L_c is thus found to exhibit a heavy tail with respect to the lognormal PDF with a two slope algebraic tail. When computing this PDF, only the data points with $L_c \leq 40$ were taken into account leaving out the inner and outer regions characterised by $L_c > 40$. On figure 8, the time trace of the inner and outer boundaries of the region with $L_c \leq 15$ are plotted. One readily observes the sudden expansion towards the end of the linear phase, followed by fluctuating positions together with large amplitude and slower

frequency modulation. Correlation and anti-correlation between the inner and outer boundary can be observed as well as different time scales for the boundary displacement. From figure 7 and figure 8, one concludes that L_c is a dynamical feature of the system, that it is specific of the chosen region within the plasma. The heavy tail structure also suggests that various events take place that are characterised by very different correlation lengths. It is then difficult to assign to this variability a single value as would have been required to readily fulfil the condition discussed in Section 2 on the scaling law.

4. Averages of the correlation length

4.1. Poloidal variation

One way to proceed towards a single characteristic value is to average the existing data despite the heavy tail PDF, figure 7. A standard procedure is the flux surface average. This allows one to reduce the space dependence to the single direction transverse to the flux surfaces. Confinement properties are then discussed in terms of profiles but it is then more problematic to seek agreement with poloidally localised measurements when poloidal dependences are expected, the ballooning structure of turbulent transport being a serious candidate for such a poloidal variation [18].

In a first step we investigate the poloidal variation of L_c assuming time homogeneity, and thus using all data points in time for the statistics. On figure 9, the poloidal dependence of the

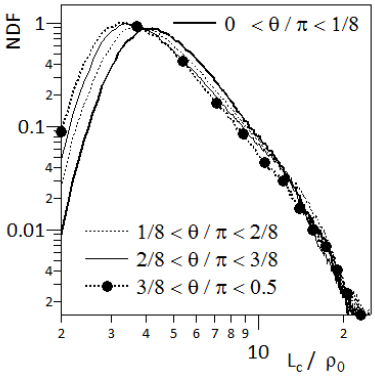

Figure 9. Poloidal dependence of the PDF, with the poloidal angle divided in 16 sectors, time coarse grained and in space such that $150 \leq r/\rho_* \leq 200$.

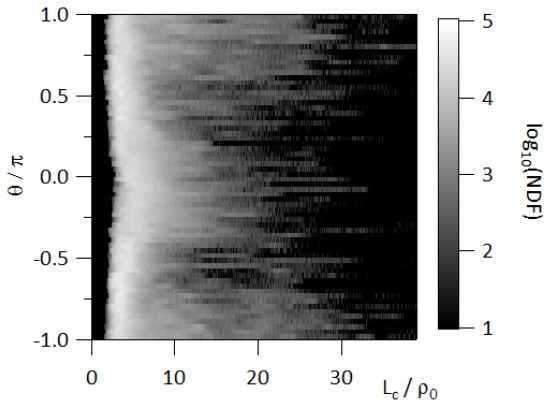

Figure 10. Poloidal distribution of the PDF, coarse grained in time, with 128 poloidal sectors and a single radial position.

PDF of L_c is shown in four different poloidal regions located on the low field side towards the top, $0 \leq \theta \leq \pi/2$. One finds that the PDF maximum is shifted towards the smaller values as θ is increasing [18]. For this plot a range of values of the radial position $150 \leq r/\rho_s \leq 200$ is used to increase the statistics. A complete poloidal dependence is illustrated on figure 10, in this case a single radial point $r/\rho = 150$ is used. These two PDFs are computed using all available points in time in the nonlinear regime. The poloidal dependence exhibits a near Top-Down symmetry, $\theta \to -\theta$. The PDF appears to be very broad with marked narrowing at $\theta \approx \pm\ \pi/4$. As already underlined, the PDF maximum decreases from the low-field midplane towards the high-field miplane. On the high-field side, the PDF appears to develop a double hump, the secondary structure building for $L_c \approx 25\ \rho_0$. From this analysis, one finds that there is no poloidal symmetry with in particular a difference between the low and high field side as expected from

the known ballooned feature of ITG turbulence.

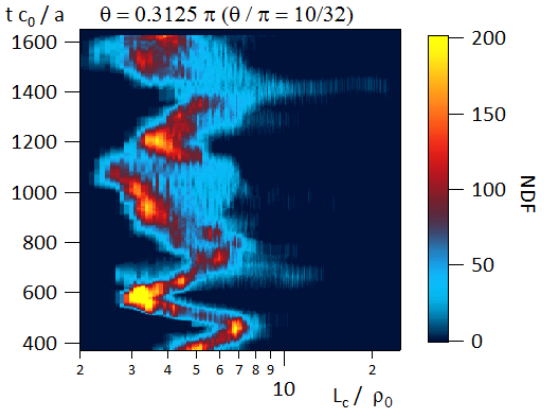

Figure 11. Contour plot of the PDF with its time evolution in the low field top sector.

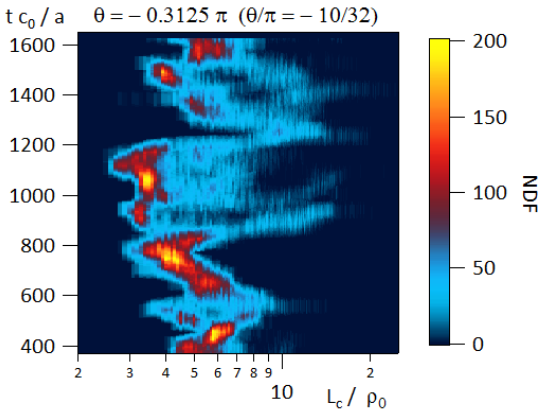

Figure 12. Contour plot of the PDF with its time evolution in the low field bottom sector.

We now address the time dependence of the PDF of L_c, see figure 11 for the low field region towards the top, and figure 12 for the low field towards the bottom. Two features are striking, first without time averaging one loses the top-bottom symmetry, second the evolution is marked by quiescent phases with narrow PDFs peaking towards the low values of the correlation length, interrupted by relaxation events with broad PDF's extending towards the large values of L_c. It thus appears that the top-down symmetry reported previously only holds when considering time averages. Furthermore, one finds that the time dependence is far from being homogeneous with qualitative and quantitative variations.

4.2. Comparing corrugation and correlation length patterns

The simulation that has been used is characterised by marked corrugation patterns [29, 30, 31, 32], see figure 13. The latter are identified as regions with large shear (both negative and positive shear of the $E \times B$ flow) and are readily identified on the contour plot figure 13 despite their variation in time, including rather high frequency behaviour, and radial position [36]. On the latter figure, one can identify two specific features; first the long lived shear patterns appear to go in pairs with a zero line separating them, second, short lived shear structure [37] appear to have a ballistic motion that is readily associated to avalanche transport [24, 25, 26, 27, 28]. The former pattern is correlated to the corrugations in the temperature gradient [29] and is in fact a double shear layer associated to a maximum or a minimum of the zonal flow, here defined as $< v_{E\theta} >_\theta$, namely the flux surface average of the poloidal component of the $E \times B$ drift velocity. Rather than defining a precise pattern of the corrugations, we define a series of points where the absolute value of the zonal flow shear goes through a local maximum in the radial direction. This data is superimposed on the 2D contour plot of the correlation length L_c plotted against radius and time, and for poloidally localised data $0 \leq \theta \leq \pi/4$, figure 14. On this figure one finds that the black dots of the shear extrema are organised in the form of corridors that bound regions of minimum correlation length, typically $L_c \leq 5$ which is the order of magnitude of the width of the local peak in zonal flow amplitude that drives the corrugation.

The corrugation pattern appears to wind around radially with time, figure 13. A time average will thus tend to smear out the correlation between the local shear regions and the minima in L_c. It will then be difficult to untangle the physics that finally yields a given average in time of

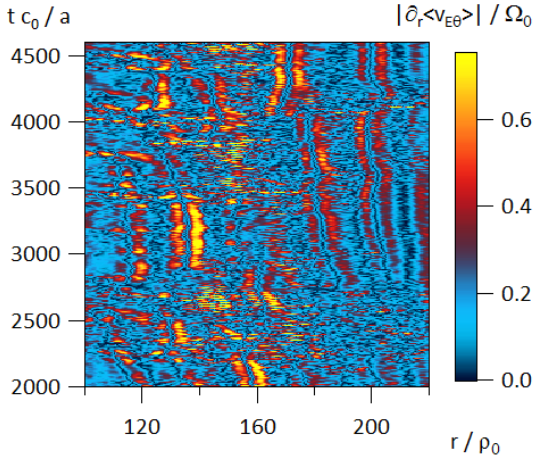

Figure 13. Contour plot of the absolute value of the zonal flow shear displaying the corrugation patterns.

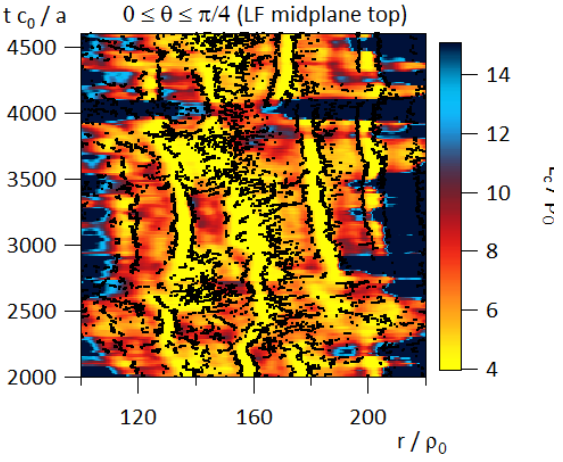

Figure 14. Contour plot of the correlation length and superimposed position (radius, time) of the local maximum of the zonal flow shear.

L_c. Furthermore, the noticeable agreement displayed on figure 14 for the low field side data of L_c vanishes and no meaningful matching is found between the shear layer pattern and that of averaged (coarse grained) L_c values. In agreement with the latter observation, one readily checks that the matching of the high field side values of L_c and the zonal flow shear is rather poor. One thus finds that the shearing effect does not act uniformly in the poloidal direction. Indeed

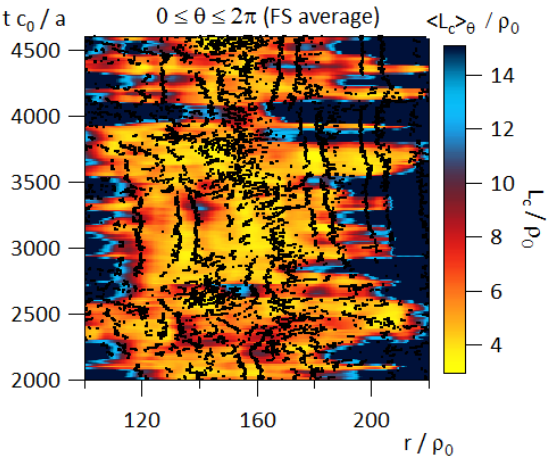

Figure 15. Contour plot of the correlation length coarse grained on a complete flux surface and superimposed position of the local maximum zonal flow shear.

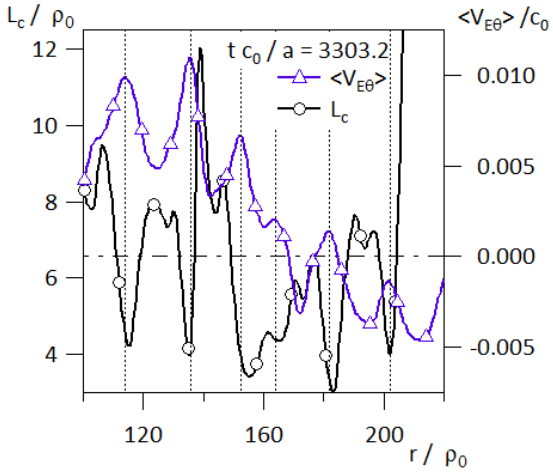

Figure 16. Profiles of the zonal flow shear and of the correlation length with matching between the maxima of the zonal flow and minima of L_c.

it appears to govern minima in the correlation length only in the low field side region. Consequently, the poloidal averaged value of L_c also falls short of reflecting the actual self-regulation of turbulent transport. Similarly, when considering the radial profiles of the correlation length, with minima aligned on the maxima of the zonal flow, figure 16, one finds that radial coarse

graining will tend to mask this alignment property.

It thus seems that the self-regulation of turbulent transport by the zonal flows is a local feature in the poloidal and radial directions which also exhibits a clear evolution. Coarse graining in order to reduce the distribution of the correlation length to a single characteristic value will thus mask this key property. The investigation of the scaling law of the energy confinement on the basis of a correlation length analysis does not appear to be as straightforward as would be the case for homogeneous turbulent systems.

5. Discussion and Conclusions

Bridging the experimental effort on confinement performance, exemplified by the empirical scaling law of the energy confinement time, to the theoretical investigation is usually based on computing correlation lengths and times. Knowing the scaling of these quantities, one can then estimate that of diffusion coefficients and consequently that of the confinement time. Gyrokinetic codes have built-in self similarity so that one readily expects the radial correlation length to scale like $1/B$ according to the gyro-Bohm scaling. However, in view of the questions opened by the empirical scaling law, it is important to investigate this result in terms of the isotope (or mass) effect as well as with other dependencies.

In that spirit we have analysed a GYSELA simulation at $1/\rho_* \approx 300$ that has been run for a large fraction of the confinement time using as input data from a Tore Supra shot. The analysis of the correlation length has indicated a very rich distribution of values with a heavy tail and double algebraic law towards the large values. The detailed analysed has revealed that the correlation length exhibits patterns that are reminiscent of that of the corrugations with minimal values of the correlation length and of its rms value located at the position of the corrugations. Furthermore, in agreement with the ballooned structure of turbulent transport the correlation length exhibits a poloidal variation. Finally, one finds that the corrugations evolve slowly in time introducing consequently a time dependence of the radial pattern of the correlation length. An interesting and unexpected result of the analysis has been the poloidally localised matching of the corrugation and correlation length patterns. Consequently, one finds that any averaging process of the correlation length, in time, poloidal angle or radius, will remove the connection between the correlation length and the self-organised turbulent transport properties.

The result of the present analysis is thus twofold: on the one hand it is difficult to define a single correlation length for a given simulation region. The standard averaging procedures in radius, poloidal angle or time suppress the correlation between confinement properties and the correlation length and as such are not appropriate. The description of confinement in terms of a random walk must then be analysed on the bases of non-homogeneous models, including anomalous transport such as trapping or sticking. This becomes a considerable task of its own that is not yet available. Further effort is thus needed to scale the PDF of the correlation lengths and correlation times with the key dimensionless control parameters. Such an analysis must also involve the scaling properties of the meso scale features such as the corrugation width and their typical radial separation. On the other hand, one finds that the experimental analysis of the transport properties and scaling laws must face the same issues. Indeed, the experimental investigation of turbulence properties yields local measurements of the correlations. The issue of comparing local properties to global confinement properties is thus the same in the experiments and the simulations. Using the latter to define the appropriate framework for such comparison should help in clarifying some of the open issues such as the isotope effect. Finally, as underlined by the analysis of the scaling law of the confinement time in the first part of the paper, consistent changes of the simulation parameters are mandatory to avoid introducing spurious correlations

within the scans that would open the way to misleading interpretation of the results.

Acknowledgments
The authors acknowledge the fruitful and lively discussions held during the Festival de Théorie in Aix-en-Provence. They are most indebted to Pat Diamond for his strong support and very active scientific participation to this event. This work is carried out in the framework of the ANR-GYPSI and ANR-ESPOIR projects (ANR-10-BLAN-941 and ANR-09-BLAN-0035-01).

References

[1] I. P. E. G. on Confinement, Transport, I. P. E. G. on Confinement Modelling, Database, and I. P. B. Editors, "Chapter2: Plasma confinement and transport," *Nuclear Fusion*, vol. 39, no. 12, p. 2175, 1999.
[2] M. Shimada, D. Campbell, V. Mukhovatov, M. Fujiwara, N. Kirneva, K. Lackner, M. Nagami, V. Pustovitov, N. Uckan, J. Wesley, N. Asakura, A. Costley, A. Donn, E. Doyle, A. Fasoli, C. Gormezano, Y. Gribov, O. Gruber, T. Hender, W. Houlberg, S. Ide, Y. Kamada, A. Leonard, B. Lipschultz, A. Loarte, K. Miyamoto, V. Mukhovatov, T. Osborne, A. Polevoi, and A. Sips, "Chapter 1: Overview and summary," *Nuclear Fusion*, vol. 47, no. 6, p. S1, 2007.
[3] F. W. Perkins, C. W. Barnes, D. W. Johnson, S. D. Scott, M. C. Zarnstorff, M. G. Bell, R. E. Bell, C. E. Bush, B. Grek, K. W. Hill, D. K. Mansfield, H. Park, A. T. Ramsey, J. Schivell, B. C. Stratton, and E. Synakowski, "Nondimensional transport scaling in the tokamak fusion test reactor: Is tokamak transport bohm or gyro?bohm?," *Physics of Fluids B: Plasma Physics (1989-1993)*, vol. 5, no. 2, pp. 477–498, 1993.
[4] J. Candy and R. E. Waltz, "Anomalous transport scaling in the diii-d tokamak matched by supercomputer simulation," *Phys. Rev. Lett.*, vol. 91, p. 045001, Jul 2003.
[5] Z. Lin, S. Ethier, T. S. Hahm, and W. M. Tang, "Size scaling of turbulent transport in magnetically confined plasmas," *Phys. Rev. Lett.*, vol. 88, p. 195004, Apr 2002.
[6] B. F. McMillan, X. Lapillonne, S. Brunner, L. Villard, S. Jolliet, A. Bottino, T. Görler, and F. Jenko, "System size effects on gyrokinetic turbulence," *Phys. Rev. Lett.*, vol. 105, p. 155001, Oct 2010.
[7] T. Vernay, S. Brunner, L. Villard, B. F. McMillan, S. Jolliet, T. M. Tran, and A. Bottino, "Synergy between ion temperature gradient turbulence and neoclassical processes in global gyrokinetic particle-in-cell simulations," *Physics of Plasmas (1994-present)*, vol. 19, no. 4, pp. –, 2012.
[8] D. Schissel, J. DeBoo, K. Burrell, J. Ferron, R. Groebner, H. S. John, R. Stambaugh, B. Tubbing, K. Thomsen, J. Cordey, M. Keilhacker, D. Stork, P. Stott, A. Tanga, and J. Team, "H-mode energy confinement scaling from the diii-d and jet tokamaks," *Nuclear Fusion*, vol. 31, no. 1, p. 73, 1991.
[9] J. Christiansen, J. Cordey, K. Thomsen, A. Tanga, J. DeBoo, D. Schissel, T. Taylor, O. Kardaun, F. Wagner, F. Ryter, S. Kaye, Y. Miura, N. Suzuki, M. Mori, T. Matsuda, H. Tamai, T. Takizuka, S.-I. Itoh, and K. Itoh, "Global energy confinement h-mode database for iter," *Nuclear Fusion*, vol. 32, no. 2, p. 291, 1992.
[10] C. C. Petty, T. C. Luce, K. H. Burrell, S. C. Chiu, J. S. deGrassie, C. B. Forest, P. Gohil, C. M. Greenfield, R. J. Groebner, R. W. Harvey, R. I. Pinsker, R. Prater, R. E. Waltz, R. A. James, and D. Wrblewski, "Nondimensional transport scaling in diii?d: Bohm versus gyro?bohm resolved," *Physics of Plasmas (1994-present)*, vol. 2, no. 6, pp. 2342–2348, 1995.
[11] C. C. Petty and T. C. Luce, "Scaling of heat transport with collisionality," *Physics of Plasmas (1994-present)*, vol. 6, no. 3, pp. 909–921, 1999.
[12] D. C. McDonald, J. G. Cordey, C. C. Petty, M. Beurskens, R. Budny, I. Coffey, M. de Baar, C. Giroud, E. Joffrin, P. Lomas, A. Meigs, J. Ongena, G. Saibene, R. Sartori, I. Voitsekhovitch, and J. E. contributors, "The beta scaling of energy confinement in elmy h-modes in jet," *Plasma Physics and Controlled Fusion*, vol. 46, no. 5A, p. A215, 2004.
[13] C. C. Petty, T. C. Luce, D. C. McDonald, J. Mandrekas, M. R. Wade, J. Candy, J. G. Cordey, V. Drozdov, T. E. Evans, J. R. Ferron, R. J. Groebner, A. W. Hyatt, G. L. Jackson, R. J. La Haye, T. H. Osborne, and R. E. Waltz, "Beta scaling of transport on the diii-d tokamak: Is transport electrostatic or electromagnetic?," *Physics of Plasmas (1994-present)*, vol. 11, no. 5, pp. 2514–2522, 2004.
[14] D. McDonald, J. Cordey, K. Thomsen, O. Kardaun, J. Snipes, M. Greenwald, L. Sugiyama, F. Ryter, A. Kus, J. Stober, J. DeBoo, C. Petty, G. Bracco, M. Romanelli, Z. Cui, Y. Liu, Y. Miura, K. Shinohara, K. Tsuzuki, Y. Kamada, T. Takizuka, H. Urano, M. Valovic, R. Akers, C. Brickley, A. Sykes, M. Walsh, S. Kaye, C. Bush, D. Hogewei, Y. Martin, A. Cote, G. Pacher, J. Ongena, F. Imbeaux, G. Hoang, S. Lebedev, A. Chudnovskiy, and V. Leonov, "Recent progress on the development and analysis of the itpa global h-mode confinement database," *Nuclear Fusion*, vol. 47, no. 3, p. 147, 2007.
[15] S. D. Scott, M. C. Zarnstorff, C. W. Barnes, R. Bell, N. L. Bretz, C. Bush, Z. Chang, D. Ernst, R. J. Fonck,

L. Johnson, E. Mazzucato, R. Nazikian, S. Paul, J. Schivell, E. J. Synakowski, H. Adler, M. Bell, R. Budny, E. Fredrickson, B. Grek, A. Janos, D. Johnson, D. McCune, H. Park, A. Ramsey, M. H. Redi, G. Taylor, M. Thompson, and R. Wieland, "Isotopic scaling of confinement in deuteriumtritium plasmas," *Physics of Plasmas (1994-present)*, vol. 2, no. 6, pp. 2299–2307, 1995.

[16] J. Cordey, B. Balet, D. Bartlett, R. Budny, J. Christiansen, G. Conway, L.-G. Eriksson, G. Fishpool, C. Gowers, J. de Haas, P. Harbour, L. Horton, A. Howman, J. Jacquinot, W. Kerner, C. Lowry, R. Monk, P. Nielsen, E. Righi, F. Rimini, G. Saibene, R. Sartori, B. Schunke, A. Sips, R. Smith, M. Stamp, D. Start, K. Thomsen, B. Tubbing, and M. von Hellermann, "Plasma confinement in jet hmode plasmas with h, d, dt and t isotopes," *Nuclear Fusion*, vol. 39, no. 3, p. 301, 1999.

[17] T. Hahm, L. Wang, W. Wang, E. Yoon, and F. Duthoit, "Isotopic dependence of residual zonal flows," *Nuclear Fusion*, vol. 53, no. 7, p. 072002, 2013.

[18] Y. Sarazin, V. Grandgirard, J. Abiteboul, S. Allfrey, X. Garbet, P. Ghendrih, G. Latu, A. Strugarek, G. Dif-Pradalier, P. Diamond, S. Ku, C. Chang, B. McMillan, T. Tran, L. Villard, S. Jolliet, A. Bottino, and P. Angelino, "Predictions on heat transport and plasma rotation from global gyrokinetic simulations," *Nuclear Fusion*, vol. 51, no. 10, p. 103023, 2011.

[19] M. Nakata and Y. Idomura, "Plasma size and collisionality scaling of ion-temperature-gradient-driven turbulence," *Nuclear Fusion*, vol. 53, no. 11, p. 113039, 2013.

[20] V. Grandgirard, Y. Sarazin, P. Angelino, A. Bottino, N. Crouseilles, G. Darmet, G. Dif-Pradalier, X. Garbet, P. Ghendrih, S. Jolliet, G. Latu, E. Sonnendrcker, and L. Villard, "Global full- f gyrokinetic simulations of plasma turbulence," *Plasma Physics and Controlled Fusion*, vol. 49, no. 12B, p. B173, 2007.

[21] Y. Idomura, H. Urano, N. Aiba, and S. Tokuda, "Study of ion turbulent transport and profile formations using global gyrokinetic full- f vlasov simulation," *Nuclear Fusion*, vol. 49, no. 6, p. 065029, 2009.

[22] S. Ku, C. Chang, and P. Diamond, "Full-f gyrokinetic particle simulation of centrally heated global itg turbulence from magnetic axis to edge pedestal top in a realistic tokamak geometry," *Nuclear Fusion*, vol. 49, no. 11, p. 115021, 2009.

[23] J. Heikkinen, S. Janhunen, T. Kiviniemi, and F. Ogando, "Full f gyrokinetic method for particle simulation of tokamak transport," *Journal of Computational Physics*, vol. 227, no. 11, pp. 5582 – 5609, 2008.

[24] Y. Sarazin, V. Grandgirard, J. Abiteboul, S. Allfrey, X. Garbet, P. Ghendrih, G. Latu, A. Strugarek, and G. Dif-Pradalier, "Large scale dynamics in flux driven gyrokinetic turbulence," *Nuclear Fusion*, vol. 50, no. 5, p. 054004, 2010.

[25] Y. Sarazin and P. Ghendrih, "Intermittent particle transport in two-dimensional edge turbulence," *Physics of Plasmas (1994-present)*, vol. 5, no. 12, pp. 4214–4228, 1998.

[26] B. F. McMillan, S. Jolliet, T. M. Tran, L. Villard, A. Bottino, and P. Angelino, "Avalanche like bursts in global gyrokinetic simulations," *Physics of Plasmas (1994-present)*, vol. 16, no. 2, p. 022310, 2009.

[27] L. Villard, A. Bottino, S. Brunner, A. Casati, J. Chowdhury, T. Dannert, R. Ganesh, X. Garbet, T. Grler, V. Grandgirard, R. Hatzky, Y. Idomura, F. Jenko, S. Jolliet, S. K. Aghdam, X. Lapillonne, G. Latu, B. F. McMillan, F. Merz, Y. Sarazin, T. M. Tran, and T. Vernay, "Gyrokinetic simulations of turbulent transport: size scaling and chaotic behaviour," *Plasma Physics and Controlled Fusion*, vol. 52, no. 12, p. 124038, 2010.

[28] S. Jolliet and Y. Idomura, "Plasma size scaling of avalanche-like heat transport in tokamaks," *Nuclear Fusion*, vol. 52, no. 2, p. 023026, 2012.

[29] G. Dif-Pradalier, P. H. Diamond, V. Grandgirard, Y. Sarazin, J. Abiteboul, X. Garbet, P. Ghendrih, A. Strugarek, S. Ku, and C. S. Chang, "On the validity of the local diffusive paradigm in turbulent plasma transport," *Phys. Rev. E*, vol. 82, p. 025401, Aug 2010.

[30] L. Villard, P. Angelino, A. Bottino, S. Brunner, S. Jolliet, B. F. McMillan, T. M. Tran, and T. Vernay, "Global gyrokinetic ion temperature gradient turbulence simulations of iter," *Plasma Physics and Controlled Fusion*, vol. 55, no. 7, p. 074017, 2013.

[31] P. Ghendrih, "Phase space structures in gyrokinetic simulations of fusion plasma turbulence." to be published in *Eur. Phys. J. D*.

[32] Norscini, "Turbulent transport close to marginal instability: role of the source driving the system out of equilibrium." 2014.

[33] P. H. Diamond, S.-I. Itoh, K. Itoh, and T. S. Hahm, "Zonal flows in plasmaa review," *Plasma Physics and Controlled Fusion*, vol. 47, no. 5, p. R35, 2005.

[34] J. Connor and J. Taylor, "Scaling laws for plasma confinement," *Nuclear Fusion*, vol. 17, no. 5, p. 1047, 1977.

[35] J.-P. Bouchaud and A. Georges, "Anomalous diffusion in disordered media: Statistical mechanisms, models and physical applications," *Physics Reports*, vol. 195, no. 45, pp. 127 – 293, 1990.

[36] E. Floriani, G. Ciraolo, P. Ghendrih, R. Lima, and Y. Sarazin, "Self-regulation of turbulence bursts and transport barriers," *Plasma Physics and Controlled Fusion*, vol. 55, no. 9, p. 095012, 2013.

[37] J. Abiteboul, P. Ghendrih, V. Grandgirard, T. Cartier-Michaud, G. Dif-Pradalier, X. Garbet, G. Latu, C. Passeron, Y. Sarazin, A. Strugarek, O. Thomine, and D. Zarzoso, "Turbulent momentum transport in core tokamak plasmas and penetration of scrape-off layer flows," *Plasma Physics and Controlled Fusion*, vol. 55, no. 7, p. 074001, 2013.